Up-regulation of autophagy by low concentration of salicylic acid delays methyl jasmonate-induced leaf senescence

Runzhu Yin[1], Jingfang Yu[1], Yingbin Ji[1,3], Jian Liu[4], Lixin Cheng[2]*, Jun Zhou[1]*

1 MOE Key Laboratory of Laser Life Science & Institute of Laser Life Science, College of Biophotonics, South China Normal University, Guangzhou 510631, China

2 Department of Critical Care Medicine, Shenzhen People's Hospital, The Second Clinical Medicine College of Jinan University, Shenzhen 518020, China

3 Luoyang Tmaxtree Biotechnology Co., Ltd, Luoyang 471023, China

4 Fujian Provincial Key Laboratory of Plant Functional Biology, College of Life Sciences, Fujian Agriculture and Forestry University, Fuzhou 350002, China

*Correspondence: Lixin Cheng, easonlcheng@gmail.com; Jun Zhou, zhoujun@scnu.edu.cn

Running Title: interaction network analysis reveals autophagy involved in LCSA signaling

ABSTRACT

Crosstalk between salicylic acid (SA) and jasmonic acid (JA) signaling plays an important role in molecular regulation of plant senescence. Our previous works found that SA could delay methyl jasmonate (MeJA)-induced leaf senescence in a concentration-dependent manner. Here, the effect of low concentration of SA (LCSA) application on MeJA-induced leaf senescence was further assessed. High-throughput sequencing (RNA-Seq) results showed that LCSA did not have dominant effects on the genetic regulatory pathways of basal metabolism like nitrogen metabolism, photosynthesis and glycolysis. The ClusterONE was applied to identify discrete gene modules based on protein-protein interaction (PPI) network. Interestingly, an autophagy-related (ATG) module was identified in the differentially expressed genes (DEGs) that exclusively induced by MeJA together with LCSA. RT-qPCR confirmed that the expression of most of the determined ATG genes were upregulated by LCSA. Remarkably, in contrast to wild type (Col-0), LCSA cannot alleviate the leaf yellowing phenotype in autophagy defective mutants (*atg5-1* and *atg7-2*) upon MeJA treatment. Confocal and western blot results showed that LCSA increased the number of autophagic bodies and autophagic flux during MeJA-induced leaf senescence. Collectively, our work revealed up-regulation of autophagy by LCSA as a key regulator to alleviate MeJA-induced leaf senescence.

Key Words: autophagy; gene modules; jasmonic acid; leaf senescence; RNA-Seq; salicylic acid

INTRODUCTION

Senescence in green plants is a complex and orderly regulated process that is crucial for transiting from nutrient assimilation to nutrient remobilization (Masclaux et al., 2000; Quirino et al., 2000; Lim et al., 2003; Yoshida, 2003; Schippers, 2015). During senescence, the most visible characteristic is leaf yellowing, which is the consequence of a succession of changes in cellular physiology including chlorophyll degradation and photosynthetic activity reduction (Lim et al., 2003; Yoshida, 2003). Chloroplast as an early senescence signaling response organelle, its dismantling plays an important role in the major nitrogen source recycling and remobilization (Avila-Ospina et al., 2014). The progression of leaf senescence can be prematurely induced by multiple environmental and endogenous factors, such as temperature, light, humidity and phytohormones (Lim et al., 2007). Hormone signaling pathways play roles at all the stages of leaf senescence, including the initiation, progression, and the terminal phases of senescence (Lim et al., 2007). Recent progresses show that senescence can be coordinately regulated by several phytohormones like cytokinins, ethylene, abscisic acid, salicylic acid (SA), and jasmonic acid (JA) (Gan and Amasino, 1995; van der Graaff et al., 2006; Hung and Kao, 2004; He et al., 2002; Morris et al., 2000). However, the detailed molecular mechanisms for these phytohormone signals in plant senescence remain poorly understood.

JA has been known as a key plant hormone for promoting senescence, based on the findings that exogenously applied methyl jasmonate (MeJA, methyl ester of JA) leads to a rapid loss of chlorophyll content and accompany with reduction of photochemical efficiency (Yue et al., 2012; Ji et al., 2016). Studies with JA-insensitive mutant *coronatine insensitive 1* (*coi1*) that exhibited defective senescence response to MeJA treatment (He et al., 2002), supporting the notion that JA signaling pathway is crucial for leaf senescence. Some other evidences indicate that SA is also involved in plant senescence (Morris et al., 2000; Chai et al., 2014). The concentration of endogenous SA increases to upregulate several senescence-associated genes during leaf senescence (Morris et al., 2000; Yoshimoto et al., 2009). However, such genetic regulatory mechanisms are abolished in plants defective in the SA signaling or biosynthetic pathway (*npr1* and *pad4* mutants, and *NahG* transgenic plants) (Morris et al., 2000). Crosstalk between MeJA and SA has been broadly documented in plant defense response, which commonly manifests as a reciprocal antagonism pattern (Thaler et al., 2012). Evidence suggests that antagonistic interactions between SA and MeJA modulate the expression of a senescence-specific transcription factor WRKY53, showing induced by SA, but repressed by MeJA (Miao and Zentgraf,

3

70 2007). Overall, mechanisms determining the specificity and coordination between SA and

71 JA still need to be further explored.

72   Most of phytohormones have both stimulatory and inhibitory effects on the growth and

73 metabolism of higher plants in a dose dependent manner. It seems that SA functions in the

74 same way on the physiological and biochemical processes of plants (Ji et al., 2016;

75 Pasternak et al., 2019). Low-concentration SA (hereafter as LCSA) at below 50 micromole

76 (µM) promotes adventitious roots and altered architecture of the root apical meristem,

77 whereas high-concentration SA (greater than 50 µM) inhibits root growth (Pasternak et al.,

78 2019). Interestingly, we previously demonstrated that MeJA-induced leaf senescence

79 could be delayed by LCSA (1-50 µM), but accelerated when the concentration higher than

80 100 µM (Ji et al., 2016). Our other related works have verified such high dose of SA greatly

81 activates NPR1 (nonexpressor of pathogenesis-related genes 1) translocation into nucleus,

82 thereby promoting leaf senescence (Chai et al., 2014). Based on the dose dependent effect

83 of SA, Pasternak et al. (2019) proposes that at low levels it acts as a developmental

84 regulator and at high levels it acts as a stress hormone.

85   Autophagy is associated with plant senescence as defective mutants display early and

86 strong yellowing leaf symptoms (Hanaoka et al., 2002; Xiong et al., 2005; Avila-Ospina et

87 al., 2014; Li et al., 2014). Autophagy negatively regulates cell death by controlling NPR1-

88 dependent SA signaling during senescence in Arabidopsis (Yoshimoto et al., 2009). The

89 senescence process always accompanies with the equilibrium between oxidative and

90 antioxidative capacities of the plant, which creates a characteristic oxidative environment

91 resulting in the production of reactive oxygen species (ROS) and more toxic derivatives

92 (Bhattacharjee, 2005). Moreover, autophagy is involved in the degradation of oxidized

93 proteins under oxidative stress conditions in Arabidopsis (Xiong et al., 2007). Actually,

94 there is a complicated interplay between ROS and autophagy, i.e., ROS can induce

95 autophagy while autophagy be able to reduce ROS production (Signorelli et al., 2009). Our

96 previous studies showed that LCSA application delays senescence by enhancing the

97 activities of antioxidant enzymes and restricting reactive oxygen species (ROS)

98 accumulation in MeJA-treated leaves (Ji et al., 2016). However, it is still unclear whether

99 autophagy pathway is implicated in the LCSA-alleviated leaf senescence.

100   Here, the interactions between SA and MeJA in plant senescence were further

101 investigated. By applying transcriptome and interaction network analysis, we identified

102 autophagy-related (ATG) gene modules. In contrast to wild type (Col-0), LCSA cannot

103 alleviate the leaf yellowing phenotype in autophagy defective mutants upon MeJA

4

104 treatment. Further results revealed that LCSA increased the number of autophagic bodies
105 and autophagic flux during MeJA-induced leaf senescence. Collectively, our work sheds
106 light on up-regulation of autophagy by LCSA is a key regulator to alleviate MeJA-induced
107 leaf senescence.

MATERIALS AND METHODS

108

Plant materials and hormone treatments

109

110 Arabidopsis plants of wild-type (WT, Col-0), *atg5-1* (SAIL_129_B07), *atg7-2* (GK-655B06)
111 and eYFP-ATG8e (Zhuang et al., 2013) were grown in a greenhouse at 22 °C with 16 h
112 light photoperiod (120 μmol quanta^{-2} m^{-2}). Phytohormones treatment was performed as
113 described by Ji et al (2016). Briefly, the 3rd and 4th rosette leaves from four weeks of plants
114 were detached and incubated in 3 mM MES buffer (pH 5.8) containing 50 μM methyl
115 jasmonate (MeJA) and/or 10 μM salicylic acid (SA). MeJA was prepared from a 50 mM
116 stock solution in ethanol. Solutions without MeJA were supplemented with equal amounts
117 of ethanol.

Photochemical efficiency and chlorophyll content measurements

118

119 The photochemical efficiency was measured with an Imaging-PAM Chlorophyll
120 Fluorometer (PAM-MINI, Walz, Germany) followed the procedure described previously
121 (Zhou et al., 2015). After dark-adapted for 1 h, parameters Fo (minimum fluorescence with
122 PSII reaction centers fully open) and Fm (maximum fluorescence after dark adaptation)
123 were acquired with a 0.8-s saturating pulse (4,000 μmol photons m^{-2} s^{-1}). The value of
124 Fv/Fm was calculated by the formulas (Fm-Fo)/Fm. Total Chlorophyll was determined as
125 reported by Coombs et al. (1987). Chlorophyll was extracted by immersion in 90% ethanol
126 at 65 °C for 2 h. The absorbance at 664 nm and 647 nm were determined with a Lambda
127 35 UV/VIS Spectrometer (Perkin-Elmer) (Zeng et al., 2016). The concentration per fresh
128 weight of leaf tissue was calculated according to the formula: micromoles of chlorophyll
129 per milliliter per gram fresh weight = 7.93(A664) + 19.53(A647). The percentages of Fv/Fm
130 and chlorophyll content are calculated relative to the initial levels of samples before
131 treatment (time zero).

RNA-Seq analysis

132

133 Detached 3rd and 4th rosette leaves from 4-week old plants were immersed in 3 mM MES
134 buffer (pH 5.8) containing 10 μM SA, 50 μM MeJA, and MeJA together with SA for 24 h.
135 Total RNA for RNA-Seq was extracted from leaves using a Hipure plant RNA kit (Magen,

136 China). Purified RNA was analyzed either using a ND-1000 Nanodrop (Thermo Fisher,

137 USA), or by agarose gel electrophoresis to determine the RNA quantity. Those RNA

138 samples with no smear seen on agarose gels, a 260/280 ratio above 2.0, and RNA integrity

139 number greater than 8.0 were used. For RNA-Seq analysis, we mixed three replication

140 samples for each treatment into one, and total RNA samples were then sent to RiboBio

141 Co., Ltd (Guangzhou, China) for sequencing. The NEBNext Poly(A) mRNA Magnetic

142 Isolation Module (NEB, USA) was used for mRNA purification. The Ultra II RNA Library

143 Prep Kit for Illumina was used for RNA library construction. The libraries were sequenced

144 as 50-bp single end reads using Illumina Hiseq2500 according to the manufacturer's

145 instructions.

Differential Expression Analysis

147 Raw read count of each gene was generated using HTSeq with union-count mode (Love

148 et al., 2014). After normalization by Reads Per Kilobase per Million mapped reads (rpkm),

149 normalized read count table was used for determining differentially expressed genes

150 (DEGs) (Anders and Huber, 2010; Cheng et al., 2016a, 2016b), which were defined as

151 those with 2-fold changes. Fold change was calculated using log2 (normalized read

152 count+1). An R package *clusterprofiler* was used to perform the functional category

153 analysis to detect the significantly enriched Gene Ontology (GO) terms (Cheng and Leung,

154 2018a, and 2018b). Significantly enriched GO terms were selected by a threshold of $p \leq$

155 0.05. Protein-protein interaction (PPI) data was obtained from the STRING database (v.10,

156 http://string-db.org) (Szklarczyk et al., 2014). To construct a high-confidence network, only

157 the PPIs with confidence scores larger than 0.7 were considered in this work. ClusterONE

158 was adopted for the identification of protein clusters or functional modules using default

159 parameters as described previously (Cheng et al., 2017; Cheng et al., 2019). The protein

160 modules including five or more than five members and having connection density over 0.5

161 are defined as modules.

RT-qPCR

163 Total RNA was isolated using Eastep Super RNA Kit (Promega, Shanghai, China) and

164 genomic DNA was removed using DNase I. 1 µg of RNA was used to make cDNA with the

165 GoScript™ Reverse Transcription System (Promega, Shanghai, China). For qPCR 10 µL

166 of Green-2-Go 2X qPCR-S Mastermix (Sangon, Shanghai, China) and 1 µL of cDNA (100

167 ng/µL) for a total of 20 µL was used in each well. Real-time PCR was done on a CFX

168 Connect Real-Time System (BioRad) at 95 °C for 2 mins, and 45 cycles of 95 °C for 15 s,

169   55 °C for 30s, and 72 °C for 30s followed by a melting curve analysis. For each sample 3

170   biological reps were used and repeated 3 times for technical replication. qPCR was

171   analyzed using the ΔΔCt method. Primers for qPCR were showed in Table S2. Statistical

172   significance was determined using Duncan's multiple range test.

Confocal microscopy

174   Detached 3rd and 4th rosette leaves were immersed in 3 mM MES buffer (pH 5.8)

175   containing 50 μM MeJA and/or 10 μM SA for 24 h. Confocal images were captured with

176   63x (numerical aperture [NA], 1.4) objective using an LSM 880 microscope (Zeiss). For

177   quantification of autophagic puncta, randomly selected 15 to 20 images for each three

178   independent experiments were quantified with ImageJ. All images were collected with the

179   same settings determined prior to the experiment to yield nonsaturating conditions.

Western Blot

181   Treatment leaves were ground in liquid nitrogen and extracted with the lysis buffer (50 mM

182   Tris-HCl, pH 7.5, 150 mM NaCl,1 mM EDTA,1% SDS, and 1x Protease Inhibitor Cocktail

183   (MCE, Medchemexpress)). The total lysate was centrifuged at 12,000g for 20 min at 4°C.

184   Protein extracts were separated using SDS-PAGE and then western blotted. Blots were

185   stained with Ponceau S to confirm even loading. A 1:10000 dilution of monoclonal rabbit

186   anti-GFP antibody (HuaAn Biotechnology, Hangzhou, China) was used. Subsequently,

187   blots were washed and incubated with an anti-Rabbit IRDye® 800CW conjugated

188   secondary antibody (Abcam).

RESULTS

LCSA delays MeJA-induced leaf senescence

191   Our previous results indicated that SA delays MeJA-induced leaf senescence in a

192   concentration-dependent manner, showing accelerated by high SA concentrations (greater

193   than 100 μM) but attenuated by low SA concentrations (1-50 μM) (Ji et al., 2016). On this

194   basis, 10 μM SA, the most effective concentration according to Ji et al., 2016, was selected

195   as low working solution to further confirm the effect of LCSA. As shown in Figure 1, in

196   contrast to control, LCSA did not appear to have a discernible effect on senescence.

197   Leaves incubated with MeJA (50 μM) were greatly turned yellow after 5 days treatment.

198   However, when MeJA worked together with LCSA (MeJA+LCSA), the leaf yellowing was

199   alleviated (Figure 1A). Consistent with the visible phenotype, the photochemical efficiency

200 Fv/Fm and loss of chlorophyll content in the leaves combined treatment with LCSA and

201 MeJA was less severe relative to that of the leaves treated with MeJA alone (Figure 1B

202 and 1C). These physiological and biochemical data is consistent with our previous finding

203 that LCSA provide protection against senescence caused by MeJA.

204 Expression patterns of genes in LCSA-induced delayed leaf senescence

205 To investigate the genome-wide effect of LCSA on MeJA-induced gene expression

206 changes, we performed RNA-sequencing experiments. Since gene transcription regulation

207 occurs prior to visible phenotype, leaves treatment with phytohormones at 1 d were

208 selected according to our previous study (Ji et al., 2016). Totally, 408, 2536 and 2800 genes

209 displayed at least 2-fold changes in the expression level of LCSA, MeJA, and MeJA+LCSA

210 -treated leaves, respectively, relative to control leaves (Figure 2A). Of these, the number

211 of differentially expressed genes (DEGs) of LCSA alone were greatly less than that in MeJA

212 or MeJA+LCSA treatment group, in consistent with the inconspicuous phenotype between

213 SA and control leaves (Figure 1). Therefore, our study is mainly concentrated on the

214 differential expression of gene between MeJA and MeJA+LCSA.

215   To interpret the upregulated and down-regulated DEGs resulting from the MeJA and

216 MeJA+LCSA treatment, functional enrichment of Gene Ontology (GO) terms was

217 performed using the hypergeometric test (P-value < 0.05). The analysis of biological

218 process GO terms illustrated that most of the induced DEGs related to amino acid

219 (Glutathione, Cyanamino acid, arginine, proline, alanine, aspartate and glutamate)

220 metabolism, nitrogen metabolism, and flavonoid biosynthesis, whereas, the repressed

221 DEGs mainly related to carbon metabolism, photosynthesis, and glycolysis (Figure 2B).

222 These features of nitrogen and carbohydrate metabolism are consistent with the senescing

223 phenotype of leaves. In contrast to MeJA alone, unexpectedly, LCSA together with MeJA

224 treatment did not make much differences on the enriched biological processes (Figure 2C).

225 The heatmap illustrated the top 50 up-regulated and down-regulated DEGs, which also

226 revealed an extremely similar expression pattern between the DEGs of MeJA and

227 MeJA+LCSA treatment (Figure 2D). These results indicated that LCSA does not appear to

228 have dominant effects on the genetic regulatory network of basal metabolism like nitrogen

229 metabolism, photosynthesis, and glycolysis.

230 Network analysis identifies autophagy-related gene module

231 Since the enrichment analysis only provided undifferentiated biological processes about

232 basal metabolism, network analysis was conducted using DEGs that induced by MeJA and

233 MeJA+LCSA, respectively. The protein-protein interactions (PPI) were collected from the

234 STRING database, and only the PPIs with confidence scores higher than 0.7 were selected,

235 resulting in a high confidence network with 719964 interactions and 17372 proteins.

236 ClusterONE was used to identify functional protein modules, which were defined by the

237 protein clusters including five or more than five members and having connection density

238 over 0.5 (Cheng et al., 2019). According to such screening specifications, we identified 15

239 gene modules in MeJA treatment group and 16 gene modules in MeJA+LCSA group,

240 respectively (Figure S1 and S2). Of these, six gene modules were specially detected in the

241 MeJA treatment group (Figure S3). Interestingly, MeJA together with SA exclusively

242 induced seven gene modules, covering genes involved in autophagy-related (ATG)

243 pathway, phytohormone response, ATP-binding cassette transporters, aquaporins, and

244 flavonoid biosynthesis (Figure 3A). In this context, autophagy is an essential intracellular

245 degradation system that plays important roles in nutrient remobilization during leaf

246 senescence (Avila-Ospina et al., 2014). We found that the transcript abundance for ATG

247 proteins (ATG4, ATG8, ATG9, and ATG12) was differentially sensitive to the MeJA+LCSA

248 treatment. From the enriched biological processes and molecular functions, we observed

249 that these ATGs are the core components that contribute to autophagosome mature and

250 biogenesis (Figure 3B and 3C). Collectively, these results suggest a framework in which

251 MeJA together with LCSA regulates the abundance of specific gene network, such as the

252 autophagy process.

253 We next investigated whether the autophagy pathway was involved in LCSA-delayed

254 leaf senescence. Ten ATG genes (ATG4A, ATG4B, ATG5, ATG6, ATG7, ATG8A, ATG8E,

255 ATG8H, ATG12A, and ATG12B) that implemented in autophagosome formation were

256 examined by RT-qPCR (Figure 4). In contrast to MeJA alone, most of these determined

257 ATG genes, except for ATG8A and ATG8E, were up-regulated by the combined treatment

258 group (MeJA+LCSA). The differential gene expression of ATG8 isoforms is possible due

259 to they have different expression pattern in distinct tissues (Hanaoka et al., 2002).

260 Interestingly, it should be mentioned that MeJA together with LCSA did not stimulate a

261 much more increase in gene expression compared with control, especially LCSA treatment

262 (Figure 4). These results indicate that restoration of ATG genes expression is closely

263 related to LCSA-delayed leaf senescence.

264 **SA-delayed leaf senescence is dependent on a functional autophagy pathway**

265 To further resolve whether autophagy pathway was crucial for LCSA-delayed leaf

266 senescence, two autophagy defective mutants (*atg5-1* and *atg7-2*), that involved in ATG8

267   lipidation during phagophore elongation (Feng et al., 2014), were analyzed upon LCSA
268   and/or MeJA treatment. In contrast to wild type (Col-0), leaves from *atg5-1* and *atg7-2*
269   mutants were showed much more yellowing after incubated with MeJA for 5 days (Figure
270   5A). As expect, the leaf yellowing phenotype was not alleviated when MeJA worked
271   together with LCSA (Figure 5A). Consistently, the photochemical efficiency Fv/Fm in the
272   *atg5-1* and *atg7-2* mutant leaves treated with MeJA+LCSA was not restored relative to that
273   of the leaves treated with MeJA (Figure 5B). Similarly, none of the two mutants had
274   recovered relative chlorophyll content as the Col-0 after combined treatment with MeJA
275   and LCSA (Figure 5C). These genetic results clearly illustrated that the protection against
276   MeJA-induced senescence by LCSA is dependent on a functional autophagy pathway.

SA increases autophagy activity upon MeJA-induced leaf senescence

278   Since autophagy pathway was verified involved in LCSA-delayed leaf senescence, we next
279   further determined the detailed autophagy activity. Wild-type Arabidopsis plants expressing
280   the eYFP-ATG8e fusion protein were subjected to LCSA and/or MeJA treatment, and the
281   effects of LCSA on autophagy activity were analyzed by confocal microscopy of the YFP
282   fluorescence. In control and LCSA treatment conditions, we observed a few fluorescent
283   punctate structures that were identified previously as ATG8-tagged autophagosomes (or
284   autophagic bodies) (Yoshimoto et al., 2004; Contento et al., 2005; Thompson et al., 2005).
285   Incubation of MeJA alone induced a slightly increase in accumulation of autophagic bodies
286   (Figure 6A). However, when the detached leaves were subjected to combined treatment
287   with MeJA and LCSA, there was a greatly increase in the fluorescent vesicles (Figure 6A).
288   The statistical results showed that the number of autophagic bodies was more than 2-fold
289   higher in MeJA+LCSA group than that of treatment with MeJA alone (Figure 6B). Western
290   blot analysis also indicated that MeJA together with SA treatment enhanced autophagic
291   flux, showing a decrease in eYFP-ATG8 compared with other treatments (Figure 6C).
292   Taken together, our observations collectively suggest that LCSA activates the autophagy
293   activity to delay MeJA-induced leaf senescence.

DISCUSSION

295   As the final stage of leaf development, leaf senescence is a complex process that involves
296   thousands of genes and multiple layers of regulation. Mechanisms governing the specificity
297   regulation of phytohormones and aoutput gene expression are therefore of great interest.
298   The primary objective of the work is to further explore the crosstalk between SA and JA
299   signaling in regulating plant leaf senescence. We have concentrated on examining the

300 mechanisms likely to underpin changes in the transcriptome in response to LCSA and/or

301 MeJA. Specifically, an autophagy module was identified from the DEGs that exclusively

302 induced by MeJA together with SA (Figure 3). Further results demonstrate that the

303 upregulation of autophagy by LCSA serves important function in alleviating MeJA-induced

304 leaf senescence (Figure 5 and 6).

305 Previously, we found that SA delays MeJA-induced leaf senescence in a concentration

306 dependent manner (Ji et al, 2016). The dosage-dependent effect of SA also has been

307 reported in plant root meristem regulation. SA at low levels (below 50 μM) promotes

308 adventitious roots and alters architecture of the root apical meristem, whereas high-

309 concentration SA (>50 μM) inhibits root growth (Pasternak et al., 2019). Such

310 discrepancies are probably due to SA acts as a developmental regulator at low levels, but

311 acts as a stress hormone at high levels (Pasternak et al., 2019). Interestingly, RNA-Seq

312 results showed that the number of DEGs in LCSA alone treatment were less than MeJA or

313 LCSA and MeJA combined treatment group (Figure 2A), which consistent with LCSA itself

314 did not have a discernible effect on senescence, showing the inconspicuous phenotype

315 between LCSA and control leaves (Figure 1). Moreover, in contrast to MeJA alone, LCSA

316 together with MeJA treatment did not make much differences on the biological process of

317 GO terms (Figure 2C). These results indicated that LCSA at low level is more likely function

318 as a signaling regulator, which does not have a marked impact on the basal metabolism at

319 least at the genetic regulatory level.

320 Autophagy promotes cell survival by adapting cells to stress conditions both in plants

321 and mammals. Recent reverse-genetic studies have revealed that autophagy is closely

322 associated with plant senescence, and autophagy defective mutants like *atg2*, *atg5* and

323 *atg7* all showed early yellowing leaf symptoms (Doelling et al., 2002; Yoshimoto et al.,

324 2009). SA is one of the most promising phytohormones that contribute to the induction of

325 autophagy under stress. It has previously been reported that autophagy negatively

326 regulates cell death by controlling NPR1-dependent SA signaling during senescence in

327 Arabidopsis (Yoshimoto et al., 2009). Here, the ClusterONE was applied to identify discrete

328 gene modules based on PPI network. We identified several modules including autophagy-

329 related network in DEGs that exclusively induced by MeJA together with LCSA (Figure 3A).

330 Importantly, the protection against MeJA-induced senescence by LCSA was abolished in

331 autophagy defective mutant *atg5-1* and *atg7-2* (Figure 5). These data strongly suggest an

332 important role for autophagy in LCSA-alleviated leaf senescence. Notably, unlike the

333 greatly increase of autophagic bodies induced by MeJA+LCSA, autophagosomes under

334 LCSA alone treatment were not statistically significant when compared with control (Figure

335 6). Nevertheless, it is worth pointing out that SA at 100 µM, a high-concentration that could

336 promote leaf senescence based on our previous study (Chai et al., 2016), greatly induced

337 autophagic structures formation (Figure S4). In this context, we speculate that LCSA might

338 be function like a priming regulator, which could initiate signal amplification and lead to a

339 robust activation of stress response upon MeJA treatment. Actually, the priming induced

340 by some plant activators (e.g. *β*-aminobutyric acid, and thiamine) are dependent on SA

341 signaling (Ahn et al., 2005; Jung et al., 2009; Zhou et al., 2013). It would be interesting to

342 test the priming effect of LCSA on leaf senescence in future research.

343   In summary, this study further investigated the interactions between SA and MeJA in

344 plant senescence. Several modules including an autophagy-related (ATG) cluster were

345 identified by analyzing the transcriptome data and protein interaction networks. Our results

346 showed that LCSA could upregulate autophagy to alleviate leaf senescence when

347 combined treatment with MeJA. This was confirmed by founding that LCSA cannot alleviate

348 the leaf yellowing phenotype in autophagy defective mutants upon MeJA treatment.

349 Collectively, our work reveals LCSA tend to function as a signaling regulator to upregulate

350 autophagy pathway, which serves as an important cellular mechanism responsible for

351 alleviation of MeJA-induced leaf senescence.

Data availability

353 RNA-seq data were deposited in the Sequence Read Archive (SRA) database
354 https://www.ncbi.nlm.nih.gov/sra with accession no. PRJNA578602.

AUTHOR CONTRIBUTIONS

356 JZ and LC designed the research. RY, JY, and YJ conducted the experiments. RY, JL, JZ
357 and LC analyzed data. JZ and LC wrote the manuscript. All authors read and approved the
358 manuscript.

CONFLICTS OF INTEREST

368 The authors declare no conflict of interest.

REFERENCES

Anders, S., Huber, W. (2010). Differential expression analysis for sequence count data. Genome Biol. 11(10), R106. doi: 10.1186/gb-2010-11-10-r106

Ahn, I. P., Kim, S., Lee, Y. H., Suh, S. C. (2007). Vitamin B1-induced priming is dependent on hydrogen peroxide and the NPR1 gene in Arabidopsis. Plant Physiol. 143(2), 838-848. doi: 10.1104/pp.106.092627

Avila-Ospina, L., Moison, M., Yoshimoto, K., Masclaux-Daubresse, C. (2014). Autophagy, plant senescence, and nutrient recycling. J. Exp. Bot. 65(14), 3799-3811. doi: 10.1093/jxb/eru039

Bhattacharjee, S. (2005). Reactive oxygen species and oxidative burst: roles in stress, senescence and signal transduction in plants. Curr. Sci. 89, 1113-1121.

Chai, J., Liu, J., Zhou, J., Xing, D. (2014). Mitogen-activated protein kinase 6 regulates NPR1 gene expression and activation during leaf senescence induced by salicylic acid. J. Exp. Bot. 65(22), 6513-6528. doi: 10.1093/jxb/eru369

Cheng, L., & Leung, K. S. (2018a). Identification and characterization of moonlighting long non-coding RNAs based on RNA and protein interactome. Bioinformatics, 34(20), 3519-3528. doi: 10.1093/bioinformatics/bty399

Cheng, L., & Leung, K. S. (2018b). Quantification of non-coding RNA target localization diversity and its application in cancers. J Mol. Cell Biol. 10(2), 130-138. doi: 10.1093/jmcb/mjy006

Cheng, L., Liu, P., Leung, K. S. (2017). SMILE: a novel procedure for subcellular module identification with localisation expansion. IET Syst. Biol. 12(2), 55-61. doi: 10.1049/iet-syb.2017.0085

Cheng, L., Liu, P., Wang, D., Leung, K. S. (2019). Exploiting locational and topological overlap model to identify modules in protein interaction networks. BMC bioinformatics, 20(1), 23. doi: 10.1186/s12859-019-2598-7

Cheng, L., Lo, L. Y., Tang, N. L., Wang, D., & Leung, K. S. (2016a). CrossNorm: a novel normalization strategy for microarray data in cancers. Sci. Rep. 6, 18898. doi: 10.1038/srep18898

Cheng, L., Wang, X., Wong, P. K., Lee, K. Y., Li, L., Xu, B., et al. (2016b). ICN: a normalization method for gene expression data considering the over-expression of informative genes. Mol. BioSyst. 12(10), 3057-3066. doi: 10.1039/c6mb00386a

Coombs. J., G. Hind, R. C. Leegood, L. L. Tieszen and A. Vonshak (1987). Analytical Techniques. In: Techniques in Bioproductivity and photosynthesis 2nd Edition. (Eds) J. Coombs, D. O. Hall, S. P. Long and J. M. O. Scurlock. 219-220. Pergamon Press.

Doelling, J. H., Walker, J. M., Friedman, E. M., Thompson, A. R., Vierstra, R. D. (2002). The APG8/12-activating enzyme APG7 is required for proper nutrient recycling and senescence in Arabidopsis thaliana. J. Biol. Chem. 277(36), 33105-33114.

Feng, Y., He, D., Yao, Z., & Klionsky, D. J. (2014). The machinery of macroautophagy. Cell Res. 24(1), 24-41. doi: 10.1038/cr.2013.168

Gan S, Amasino RM. 1995. Inhibition of leaf senescence by autoregulated production of cytokinin. Science 270:1986-1988. doi: 10.1126/science.270.5244.1986

Ji, Y., Liu, J., Xing, D. (2016). Low concentrations of salicylic acid delay methyl jasmonate-induced leaf senescence by up-regulating nitric oxide synthase activity. J.

413   Exp. Bot. 67(17), 5233-5245. doi: 10.1093/jxb/erw280

414 Jung, H. W., Tschaplinski, T. J., Wang, L., Glazebrook, J., Greenberg, J. T. (2009).
415   Priming in systemic plant immunity. Science, 324(5923), 89-91. doi:
416   10.1126/science.1170025

417 Hanaoka, H., Noda, T., Shirano, Y., Kato, T., Hayashi, H., Shibata, D., et al. (2002). Leaf
418   senescence and starvation-induced chlorosis are accelerated by the disruption of an
419   Arabidopsis autophagy gene. Plant Physiol. 129(3), 1181-1193. doi:
420   10.1104/pp.011024

421 He, Y., Fukushige, H., Hildebrand, D.F., Gan, S. 2002. Evidence supporting a role of
422   jasmonic acid in Arabidopsis leaf senescence. Plant Physiol. 128(3), 876-884. doi:
423   10.1104/pp.010843

424 Hung, K.T., Kao, C.H. 2004. Hydrogen peroxide is necessary for abscisic acid-induced
425   senescence of rice leaves. J. Plant Physiol. 161(12), 1347-1357. doi:
426   10.1016/j.jplph.2004.05.011

427 Li, F., Chung, T., Vierstra, R. D. (2014). AUTOPHAGY-RELATED11 plays a critical role in
428   general autophagy-and senescence-induced mitophagy in Arabidopsis. Plant Cell
429   26(2), 788-807. doi: 10.1105/tpc.113.120014

430 Love, M. I., Huber, W., Anders, S. (2014). Moderated estimation of fold change and
431   dispersion for RNA-seq data with DESeq2. Genome Biol. 15(12), 550. doi:
432   10.1186/s13059-014-0550-8

433 Lim, P.O., Woo, H.R., & Nam, H.G. (2003). Molecular genetics of leaf senescence in
434   Arabidopsis. Trends Plant Sci. 8(6), 272-278. doi: 10.1016/S1360-1385(03)00103-1

435 Lim, P.O., Kim, H.J., Nam, H.G. 2007. Leaf senescence. Annu. Rev. Plant Biol. 58, 115-
436   136. doi: 10.1146/annurev.arplant.57.032905.105316

437 Masclaux, C., Valadier, M.H., Brugiere, N., Morot-Gaudry, J.F., Hirel, B. 2000.
438   Characterization of the sink/source transition in tobacco (*Nicotiana tabacum* L.)
439   shoots in relation to nitrogen management and leaf senescence. Planta 211, 510-
440   518. doi: 10.1007/s004250000310

441 Miao Y., Zentgraf U. 2007. The antagonist function of Arabidopsis WRKY53 and
442   ESR/ESP in leaf senescence is modulated by the jasmonic and salicylic acid
443   equilibrium. Plant Cell 19, 819-830. doi: 10.1105/tpc.106.042705

444 Morris, K., Mackerness, S.A., Page, T., John, C.F., Murphy, A.M., et al. 2000. Salicylic
445   acid has a role in regulating gene expression during senescence. Plant J. 23:677-
446   685. doi: 10.1046/j.1365-313x.2000.00836.x

447 Pasternak, T., Groot, E. P., Kazantsev, F. V., Teale, W., Omelyanchuk, N., Kovrizhnykh,
448   V., et al. (2019). Salicylic acid affects root meristem patterning via auxin distribution
449   in a concentration-dependent manner. Plant Physiol. 180(3), 1725-1739. doi:
450   10.1104/pp.19.00130

451 Quirino, B.F., Noh, Y.S., Himelblau, E., Amasino, R.M. (2000). Molecular aspects of leaf
452   senescence. Trends Plant Sci. 5(7), 278-282. doi: 10.1016/S1360-1385(00)01655-1

453 Schippers, J.H. (2015). Transcriptional networks in leaf senescence. Curr. Opin. Plant
454   Biol. 27, 77-83. doi: 10.1016/j.pbi.2015.06.018

455 Szklarczyk, D., Franceschini, A., Wyder, S., Forslund, K., Heller, D., Huerta-Cepas, J., et
456   al. (2014). STRING v10: protein–protein interaction networks, integrated over the

457   tree of life. Nucleic Acids Res. 43(1), 447-452. doi: 10.1093/nar/gku1003

458   Thaler, J. S., Humphrey, P. T., & Whiteman, N. K. (2012). Evolution of jasmonate and

459   salicylate signal crosstalk. Trends Plant Sci. 17(5), 260-270. doi:

460   10.1016/j.tplants.2012.02.010

461   van der Graaff, E., Schwacke, R., Schneider, A., Desimone, M., Flugge, U.I., Kunze, R.

462   2006. Transcription analysis of Arabidopsis membrane transporters and hormone

463   pathways during developmental and induced leaf senescence. Plant Physiol.

464   141:776-792. doi: 10.1104/pp.106.079293

465   Xiong, Y., Contento, A. L., Bassham, D. C. (2005). AtATG18a is required for the formation

466   of autophagosomes during nutrient stress and senescence in Arabidopsis thaliana.

467   Plant J. 42(4), 535-546. doi: 10.1111/j.1365-313X.2005.02397.x

468   Xiong, Y., Contento, A. L., Nguyen, P. Q., Bassham, D. C. (2007). Degradation of

469   oxidized proteins by autophagy during oxidative stress in Arabidopsis. Plant Physiol.

470   143(1), 291-299. doi: 10.1104/pp.106.092106

471   Yoshida, S. (2003). Molecular regulation of leaf senescence. Curr. Opin. Plant Biol. 6(1),

472   79-84. doi: 10.1016/S1369526602000092

473   Yoshimoto, K., Jikumaru, Y., Kamiya, Y., Kusano, M., Consonni, C., Panstruga, R., et al.

474   (2009). Autophagy negatively regulates cell death by controlling NPR1-dependent

475   salicylic acid signaling during senescence and the innate immune response in

476   Arabidopsis. Plant Cell, 21(9), 2914-2927. doi: 10.1105/tpc.109.068635

477   Yue, H., Nie, S., Xing, D. (2012). Over-expression of Arabidopsis Bax inhibitor-1 delays

478   methyl jasmonate-induced leaf senescence by suppressing the activation of MAP

479   kinase 6. J. Exp. Bot. 63(12), 4463-4474. doi: 10.1093/jxb/ers122

480   Zeng, L., Wang, Y., Zhou, J. (2016). Spectral analysis on origination of the bands at 437

481   nm and 475.5 nm of chlorophyll fluorescence excitation spectrum in Arabidopsis

482   chloroplasts. Luminescence, 31(3), 769-774. doi: 10.1002/bio.3022

483   Zhou, J., Sun, A., Xing, D. (2013). Modulation of cellular redox status by thiamine-

484   activated NADPH oxidase confers Arabidopsis resistance to *Sclerotinia sclerotiorum*.

485   J. Exp. Bot. 64(11), 3261-3272. doi: 10.1093/jxb/ert166

486   Zhou, J., Zeng, L., Liu, J., Xing, D. (2015). Manipulation of the xanthophyll cycle

487   increases plant susceptibility to *Sclerotinia sclerotiorum*. PLoS Pathog. 11(5),

488   e1004878. doi: 10.1371/journal.ppat.1004878

489   Zhuang, X., Wang, H., Lam, S. K., Gao, C., Wang, X., Cai, Y., Jiang, L. (2013). A BAR-

490   domain protein SH3P2, which binds to phosphatidylinositol 3-phosphate and ATG8,

491   regulates autophagosome formation in Arabidopsis. Plant Cell, 25(11), 4596-4615.

492   doi: 10.1105/tpc.113.118307

493

FIGURE LEGENDS

Figure 1. LCSA alleviates MeJA-induced leaf senescence. (A) Phenotypes of detached leaves under LCSA and/or MeJA treatments. The 3rd and 4th rosette leaves were incubated in 3 mM MES buffer (pH 5.8) containing LCSA (10 μM) or MeJA (50 μM) alone or in combination (MeJA+LCSA) under continuous light for 5 d. (B and C) Measurement of the maximum quantum efficiency of photosystem II (PSII) photochemistry (Fv/Fm) (B) and total chlorophyll content (C) after LCSA and/or MeJA treatments. The percentages of Fv/Fm and chlorophyll content are relative to the initial levels at time zero. Data are the mean ± SE of three independent experiments. Different letters indicate statistically significant differences between each treatment (Duncan's multiple range test, p < 0.05).

Figure 2. RNA-Seq analyses of differentially expressed genes (DEGs) in samples treated with LCSA, MeJA and LCSA+MeJA. (A) Venn diagram showing the overlap of DEGs between LCSA, MeJA and LCSA+MeJA-treated samples. (B and C) The pathway enrichment analysis of up or down -regulated DEGs induced by MeJA alone (B) or LCSA+MeJA (C). (D) The heatmap showing expression of top 50 up-regulated and down-regulated DEGs between MeJA and MeJA+LCSA treatment group.

Figure 3. Network analysis identifies distinct signal modules in the DEGs exclusively induced by LCSA+MeJA treatment. (A) Interconnected clusters enriched among the 889 genes and their interactions with neighboring genes. The autophagy specific module was drawn in a red dotted line. Genes are colored in red if they are induced and in blue if they are repressed. (B and C) Biological process (B) and molecular function (C) classification in gene ontology analysis of the DEGs that identified in coexpression networks.

Figure 4. RT-qPCR confirmation of differentially expressed genes that involved in regulation of autophagy. The relative mRNA expression levels were calculated using the ΔΔCt method. The value of each ATG genes were relative to the initial levels at time zero of treatment. Data were the mean ± SE of three independent experiments. Different letters in each genes indicate statistically significant differences between the treatments (Duncan's multiple range test, p<0.05).

Figure 5. Defective in autophagy restrains the effect of SA on the senescence symptoms. (A) Phenotypes of LCSA-alleviated senescence in Col-0 and autophagy defective mutants (*atg5-1* and *atg7-2*). Detached leaves form four-week-old Col-0, *atg5-1*, and *atg7-2* plants were transferred to MES buffer (pH 5.8) containing LCSA (10 μM) or MeJA (50 μM) or both MeJA and LCSA under continuous light and photographs were taken after 5 days of treatment. (B and C) Relative Fv/Fm (B) chlorophyll levels (C) in the leaves of the Col-0, *atg5-1*, and *atg7-2* described in (A). The data are means ± SD (n = 3) calculated from three biological replicates. Different letters indicate statistically significant differences between the treatments (Duncan's multiple range test, p<0.05).

Figure 6. LCSA enhances the formation of autophagosomes upon MeJA-induced leaf senescence. (A) Microscopic analyses of autophagosome-related structures in the eYFP-ATG8e plant under LCSA or MeJA or both MeJA and LCSA treatment. Bar, 20 μm. (B) Statistical analysis of the puncta numbers displayed in (A). The number of puncta was

16

535   calculated per 0.01 mm^2 from at least 15 pictures. Different letters indicate statistically

536   significant differences between the treatments (Duncan's multiple range test, p<0.05). (C)

537   Immunoblot analysis of eYFP-ATG8 processing. Crude extracts were subjected to SDS-

538   PAGE and immunoblot analysis with anti-GFP antibodies. The amount of protein loaded

539   per lane was stained by ponceau S.

540   **SUPPLEMENTARY MATERIALS**

541   **Figure S1. Network analysis identifies gene modules in the DEGs induced by MeJA.**

542   Protein modules were identified using ClusterONE, a cluster screen method considering

543   the overlapping neighbor extension. The protein modules including five or more than five

544   members and having connection density over 0.5 are defined as modules.

545   **Figure S2. Network analysis identifies gene modules in the DEGs induced by MeJA**

546   **together with LCSA.** Protein modules were identified using ClusterONE. The protein

547   modules including at least five members and having connection density over 0.5 are

548   defined as modules.

549   **Figure S3. Gene modules exclusively induced by MeJA.** After removal of the same

550   modules in MeJA+LCSA treatment group, six gene modules specially induced by MeJA

551   were obtained.

552   **Figure S4. Effect of different concentrations of SA on autophagic puncta induction.**

553   (A) Microscopic analyses of autophagic structures in the eYFP-ATG8e plant under 0, 10

554   and 100 M SA treatment. Bar, 20 μm. (B) Statistical analysis of the puncta numbers

555   displayed in (A). The number of puncta was calculated per 0.01 mm^2 from at least 15

556   pictures. Asterisks indicate a significant difference according to Student's t-test, **P<0.01.

557   **Table S1. Genes list for enriched modules in the DEGs induced by MeJA and MeJA**

558   **together with LCSA.**

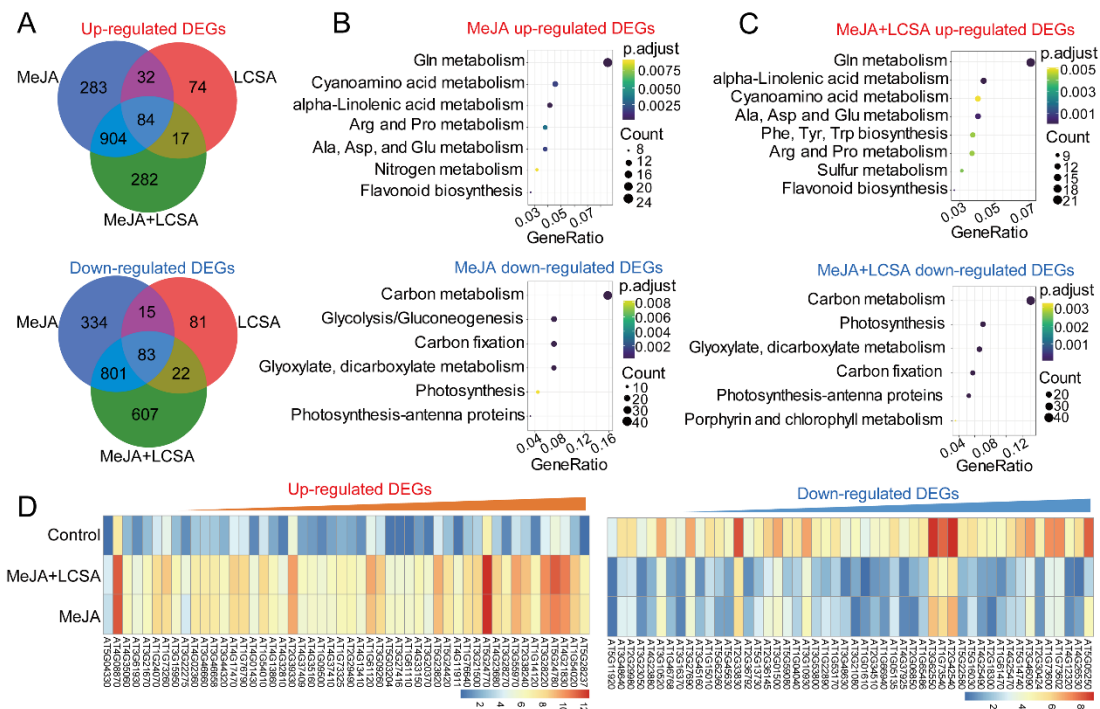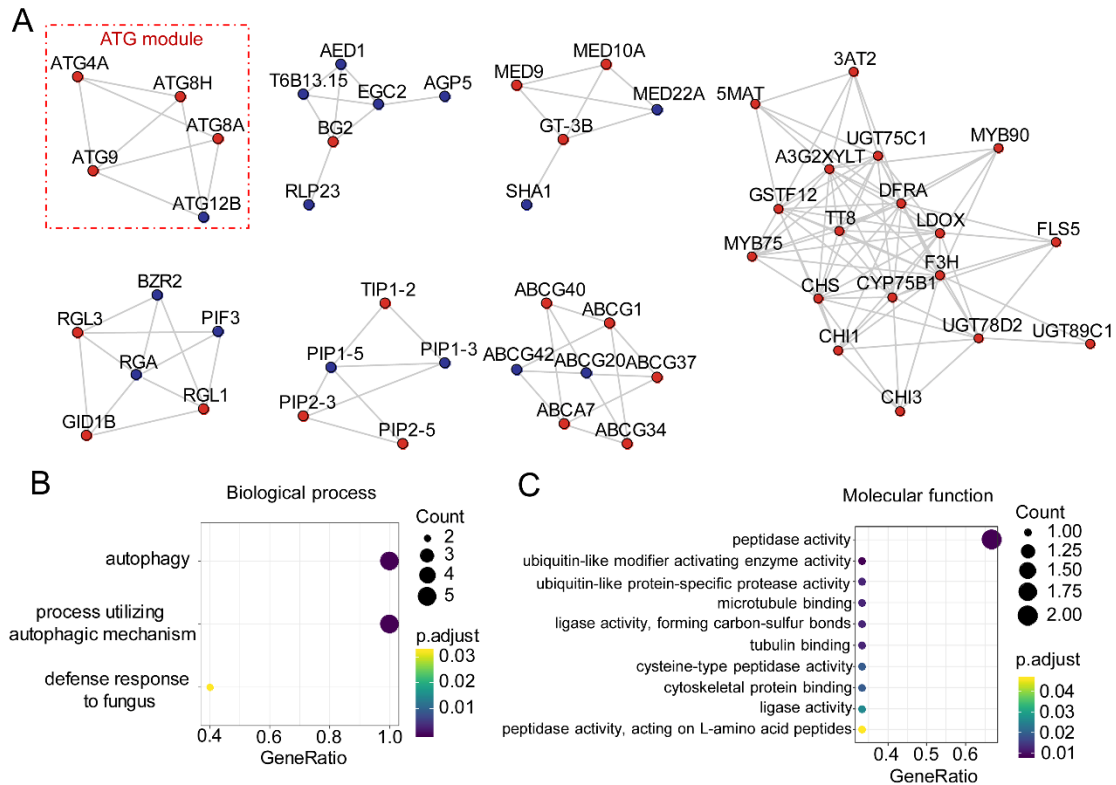559   **Table S2. Primers used for RT-qPCR.** F, Forward; R, Reverse.

560

561

Figure 1. LCSA alleviates MeJA-induced leaf senescence. (A) Phenotypes of detached leaves under LCSA and/or MeJA treatments. The 3rd and 4th rosette leaves were incubated in 3 mM MES buffer (pH 5.8) containing LCSA (10 μM) or MeJA (50 μM) alone or in combination (MeJA+LCSA) under continuous light for 5 d. (B and C) Measurement of the maximum quantum efficiency of photosystem II (PSII) photochemistry (Fv/Fm) (B) and total chlorophyll content (C) after LCSA and/or MeJA treatments. The percentages of Fv/Fm and chlorophyll content are relative to the initial levels at time zero. Data are the mean ± SE of three independent experiments. Different letters indicate statistically significant differences between each treatment (Duncan's multiple range test, $p < 0.05$).

571

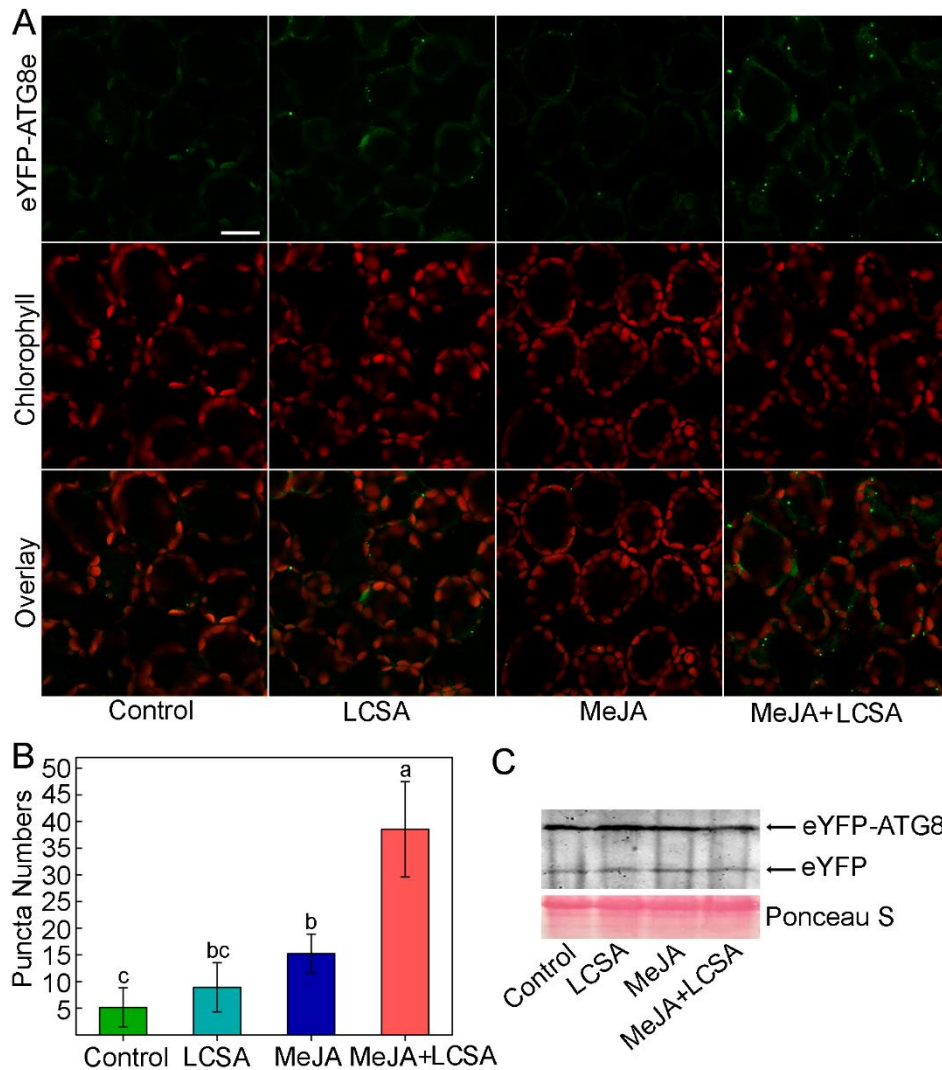**Figure 2. RNA-Seq analyses of differentially expressed genes (DEGs) in samples treated with LCSA, MeJA and LCSA+MeJA.** (A) Venn diagram showing the overlap of DEGs between LCSA, MeJA and LCSA+MeJA-treated samples. (B and C) The pathway enrichment analysis of up or down -regulated DEGs induced by MeJA alone (B) or LCSA+MeJA (C). (D) The heatmap showing expression of top 50 up-regulated and down-regulated DEGs between MeJA and MeJA+LCSA treatment group.

580

Figure 3. Network analysis identifies distinct signal modules in the DEGs exclusively induced by LCSA+MeJA treatment. (A) Interconnected clusters enriched among the 889 genes and their interactions with neighboring genes. The autophagy specific module was drawn in a red dotted line. Genes are colored in red if they are induced and in blue if they are repressed. (B and C) Biological process (B) and molecular function (C) classification in gene ontology analysis of the DEGs that identified in coexpression networks.

588

Figure 4. RT-qPCR confirmation of differentially expressed genes that involved in regulation of autophagy. The relative mRNA expression levels were calculated using the ΔΔCt method. The value of each ATG genes were relative to the initial levels at time zero of treatment. Data were the mean ± SE of three independent experiments. Different letters in each genes indicate statistically significant differences between the treatments (Duncan's multiple range test, p<0.05).

Figure 5. Defective in autophagy restrains the effect of SA on the senescence symptoms. (A) Phenotypes of LCSA-alleviated senescence in Col-0 and autophagy defective mutants (*atg5-1* and *atg7-2*). Detached leaves form four-week-old Col-0, *atg5-1*, and *atg7-2* plants were transferred to MES buffer (pH 5.8) containing LCSA (10 µM) or MeJA (50 µM) or both MeJA and LCSA under continuous light and photographs were taken after 5 days of treatment. (B and C) Relative Fv/Fm (B) chlorophyll levels (C) in the leaves of the Col-0, *atg5-1*, and *atg7-2* described in (A). The data are means ± SD (n = 3) calculated from three biological replicates. Different letters indicate statistically significant differences between the treatments (Duncan's multiple range test, p<0.05).

22

**Figure 6. LCSA enhances the formation of autophagosomes upon MeJA-induced leaf senescence.** (A) Microscopic analyses of autophagosome-related structures in the eYFP-ATG8e plant under LCSA or MeJA or both MeJA and LCSA treatment. Bar, 20 µm. (B) Statistical analysis of the puncta numbers displayed in (A). The number of puncta was calculated per 0.01 mm^2 from at least 15 pictures. Different letters indicate statistically significant differences between the treatments (Duncan's multiple range test, $p<0.05$). (C) Immunoblot analysis of eYFP-ATG8 processing. Crude extracts were subjected to SDS-PAGE and immunoblot analysis with anti-GFP antibodies. The amount of protein loaded per lane was stained by ponceau S.

619   **SUPPLEMENTARY MATERIALS**
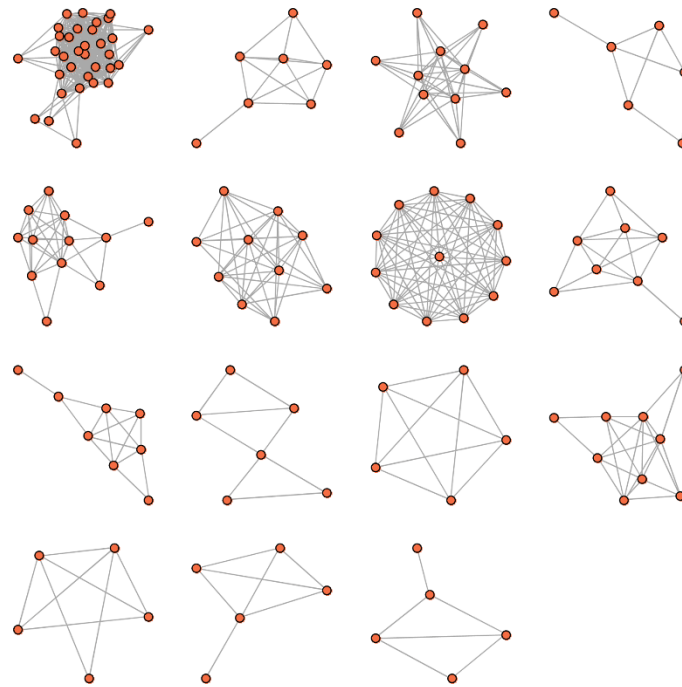
620

621   **Figure S1. Network analysis identifies gene modules in the DEGs induced by MeJA.**

622   Protein modules were identified using ClusterONE, a cluster screen method considering

623   the overlapping neighbor extension. The protein modules including five or more than five

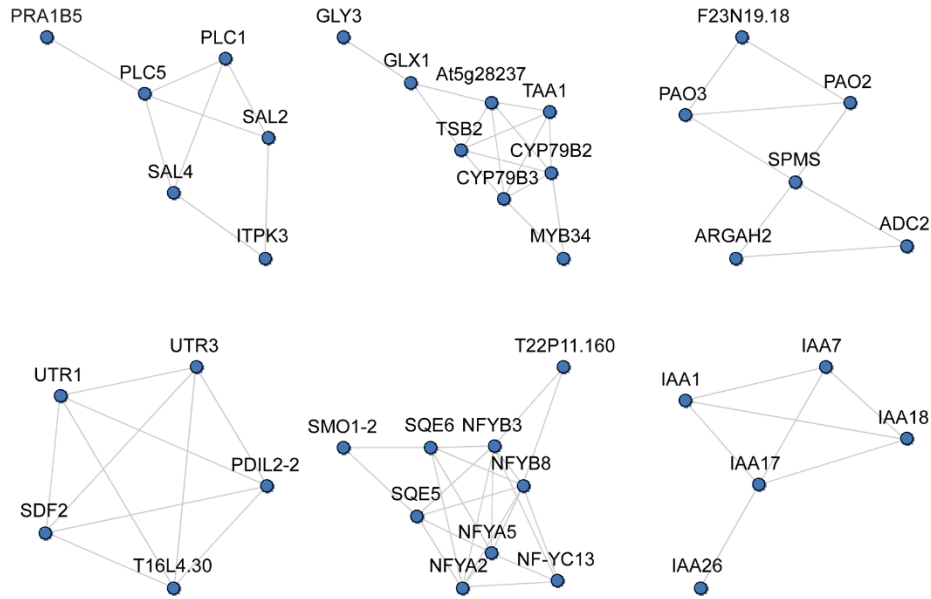624   members and having connection density over 0.5 are defined as modules.

625

Figure S2. Network analysis identifies gene modules in the DEGs induced by MeJA together with LCSA. Protein modules were identified using ClusterONE. The protein modules including at least five members and having connection density over 0.5 are defined as modules.
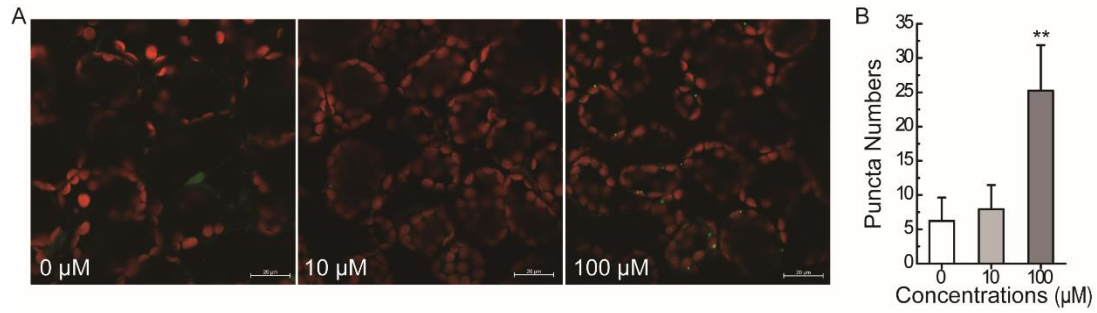
Figure S3. Gene modules exclusively induced by MeJA. After removal of the same modules in MeJA+LCSA treatment group, six gene modules specially induced by MeJA were obtained.

637

Figure S4. Effect of different concentrations of SA on autophagic puncta induction.
(A) Microscopic analyses of autophagic structures in the eYFP-ATG8e plant under 0, 10
and 100 M SA treatment. Bar, 20 µm. (B) Statistical analysis of the puncta numbers
displayed in (A). The number of puncta was calculated per 0.01 mm^2 from at least 15
pictures. Asterisks indicate a significant difference according to Student's t-test, **P<0.01.

643

644 **Table S1. Genes list for enriched modules in the DEGs induced by MeJA and MeJA**
645 **together with LCSA.**

Modules	Enriched genes in each module
MeJA_1	AT1G64200 ATCG00120 ATCG00480 ATCG00140 ATCG00190 ATCG00740 ATCG00170 ATCG00340 AT3G48850 ATCG00660 ATCG01070 ATCG01110 ATCG00420 ATCG01050 ATCG00490 AT5G24120 ATCG00280 ATCG00510 AT5G13730 ATCG01010 ATCG01100 ATMG01320 ATCG00570 ATCG00550 ATCG00710 ATCG00210 AT5G13490 ATCG00560 ATCG00040 ATCG00590 ATCG00760 ATCG00300 ATCG00700
MeJA_2	AT4G36990 AT3G24520 AT3G51910 AT3G53230 AT5G37670 AT2G20560 AT1G08650
MeJA_3	AT3G50740 AT4G36220 AT5G04330 AT3G19450 AT4G37990 AT1G71695 AT5G64120 AT3G49120 AT4G21960 AT4G08770 AT5G06720
MeJA_4	AT5G58690 AT5G58670 AT5G01640 AT4G08170 AT5G64000 AT5G09290
MeJA_5	AT1G30135 AT1G74950 AT5G13220 AT3G17860 AT1G70700 AT1G17380 AT3G43440 AT2G27690 AT2G34600 AT5G05600 AT1G44350 AT5G63450
MeJA_6	AT3G29320 AT5G64860 AT5G04360 AT3G20440 AT2G36390 AT5G51820 AT1G76130 AT4G25000 AT2G39930 AT4G00490
MeJA_7	AT3G48360 AT3G26230 AT3G26300 AT4G37400 AT1G13100 AT4G37310 AT5G57220 AT4G37320 AT4G37430 AT5G36220 AT3G53280 AT4G37410
MeJA_8	AT1G19670 AT5G43860 AT4G13250 AT5G13800 AT4G22920 AT3G44880 AT3G10520 AT4G11910
MeJA_9	AT1G70560 AT1G11840 AT5G28237 AT4G27070 AT1G53580 AT4G39950 AT2G22330 AT5G60890
MeJA_10	AT5G53120 AT1G62810 AT2G43020 AT3G59050 AT4G08870 AT4G34710
MeJA_11	AT1G04980 AT1G14360 AT2G02810 AT2G25110 AT4G29520
MeJA_12	AT5G02570 AT5G43250 AT4G22756 AT5G24160 AT5G24150 AT4G14540 AT2G37060 AT3G05690 AT1G54160
MeJA_13	AT1G02470 AT2G43018 AT3G59052 AT5G10690 AT2G06005
MeJA_14	AT1G51950 AT3G23050 AT1G04250 AT4G14560 AT3G16500
MeJA_15	AT1G52400 AT4G19230 AT3G16470 AT1G52410 AT5G24780
MeJA+LCSA_1	ATCG00470 ATCG00130 AT2G25610 AT1G64200 ATCG00120 ATCG00480 ATCG00150 ATCG00140 ATCG00770 ATCG00740 ATCG00170 ATCG00670 ATCG00020 ATCG00630 ATCG01060 AT3G48850 ATCG00650 ATCG00660 ATCG00640 ATCG01070 ATCG00430 ATCG00420 ATCG01080 ATCG01050 ATCG00490 ATCG00540 ATCG00080 ATCG00580 ATCG00070 ATCG00510 AT1G16780 AT3G27240 AT3G53920 ATCG01100 AT2G07689

28

	ATCG00440 ATCG01040 ATCG01020 ATCG00570 ATCG00550 ATCG00360 ATCG00520 ATCG00710 ATCG00210 AT5G13490 ATCG00220 ATCG00560 ATCG00040 ATCG00590 ATCG00760 ATCG00530 ATCG00700
MeJA+LCSA_2	AT1G52400 AT4G19230 AT3G16470 AT1G52410 AT5G24780
MeJA+LCSA_3	AT1G03495 AT4G14090 AT5G42800 AT5G54060 AT5G17220 AT3G29590 AT1G06000 AT3G51240 AT5G17050 AT5G13930 AT4G09820 AT4G22880 AT5G07990 AT5G63600 AT1G56650 AT1G66390 AT5G05270 AT3G55120
MeJA+LCSA_4	AT1G14540 AT5G40150 AT3G50740 AT4G36220 AT5G04330 AT4G37990 AT1G14550 AT1G71695 AT5G64120 AT3G49120 AT4G21960 AT5G05340
MeJA+LCSA_5	AT1G01260 AT1G30135 AT1G74950 AT1G72450 AT5G13220 AT3G17860 AT1G70700 AT1G17380 AT2G27690 AT2G34600 AT5G05600 AT1G44350 AT5G63450
MeJA+LCSA_6	AT1G19670 AT4G13250 AT5G13800 AT4G22920 AT3G44880 AT3G10520 AT4G11910
MeJA+LCSA_7	AT3G29320 AT5G64860 AT2G36390 AT5G03650 AT1G76130 AT4G25000 AT2G39930 AT4G00490
MeJA+LCSA_8	AT4G36990 AT3G24520 AT3G51910 AT1G77570 AT3G53230 AT1G57870 AT1G08650 AT1G73570 AT1G65040
MeJA+LCSA_9	AT1G09530 AT1G19350 AT2G01570 AT5G17490 AT1G66350 AT3G63010
MeJA+LCSA_10	AT3G26230 AT2G30750 AT4G37310 AT3G26220 AT5G57220 AT4G37320 AT4G37430 AT5G36220 AT4G37410
MeJA+LCSA_11	AT1G35230 AT2G18660 AT5G10760 AT3G57260 AT2G14610 AT2G32680
MeJA+LCSA_12	AT1G02470 AT2G43018 AT3G59052 AT5G10690 AT1G51402
MeJA+LCSA_13	AT1G16430 AT5G41910 AT2G38250 AT1G55080 AT5G63780
MeJA+LCSA_14	AT4G21980 AT3G06420 AT2G44140 AT2G31260 AT3G13970
MeJA+LCSA_15	AT1G01620 AT4G23400 AT3G26520 AT2G37180 AT3G54820
MeJA+LCSA_16	AT2G39350 AT3G47780 AT3G53510 AT1G15520 AT4G15233 AT2G36380 AT3G53480

646

647

648 **Table S2. Primers used for RT-qPCR.** F, Forward; R, Reverse.

Primer name	Sequence (5'--->3')
Actin2-F	GGCAAGTCATCACGATTGG
Actin2-R	CAGCTTCCATTCCCACAAAC
ATG4A-F	GGCTGCATTGCAACTAGATTT
ATG4A-R	GAATCATGCAACCCCAGTTC
ATG4B-F	CTTTCACGTTCCCTCAAAGC
ATG4B-R	TTGCAATGGTAAGACGATGTG
ATG5-F	GACAGCAAGAATTCCTGTTCG
ATG5-R	GGAACTCAACAGGGCGATTA
ATG6-F	GCCATGACACTGTATTTGATG
ATG6-R	TGGTCCAACTCTCTTGCTTG
ATG7-F	GTACCGCTTGCTCTGAAACC
ATG7-R	GTCTTCCCAGTCGAGGTTGA
ATG8A-F	CAATTTGTATACGTGGTTCGT
ATG8A-R	AGCAACGGTAAGAGATCCAA
ATG8E-F	GGAAGCATCTTTAAGATGGACA
ATG8E-R	CTCAGCCTTTTCCACAATCA
ATG8H-F	CCAAAGCTCTCTTTGTTTTCG
ATG8H-R	AAGAACCCGTCTTCTTCCTTG
ATG12A-F	CGAGCTCTGTTCGGAAAGTT
ATG12A-R	CAACGAATCAGAATGAAGCTG
ATG12B-F	CCGAATCTCCGAATTCTGTT
ATG12B-R	GCAAACTTGTCACTCCCTGA

649